

# K-shell photoionization of ground-state Li-like boron ions $[B^{2+}]$ : Experiment and Theory

A Müller<sup>1</sup>, S Schippers<sup>1</sup>, R A Phaneuf<sup>2</sup>, S W J Scully<sup>2,3</sup>, A Aguilar<sup>2,4</sup>, C Cisneros<sup>5</sup>, M F Gharraibeh<sup>2†</sup>, A S Schlachter<sup>4</sup>, and B M McLaughlin<sup>3,6‡</sup>

<sup>1</sup>Institut für Atom- und Molekülphysik, Justus-Liebig-Universität Giessen, 35392 Giessen, Germany

<sup>2</sup>Department of Physics, University of Nevada, Reno, Nevada 89557, USA

<sup>3</sup>Centre for Theoretical Atomic, Molecular and Optical Physics (CTAMOP), School of Mathematics and Physics, The David Bates Building, 7 College Park, Queen's University Belfast, Belfast BT7 1NN, UK

<sup>4</sup>Advanced Light Source, Lawrence Berkeley National Laboratory, Berkeley, California 94720, USA

<sup>5</sup>Centro de Ciencias Físicas, Universidad Nacional Autónoma de México, Apartado Postal 6-96, Cuernavaca 62131, Mexico

<sup>6</sup>Institute for Theoretical Atomic and Molecular Physics, Harvard Smithsonian Center for Astrophysics, MS-14, Cambridge, Massachusetts 02138, USA

**Abstract.** Absolute cross sections for the K-shell photoionization of ground-state Li-like boron  $[B^{2+}(1s^2 2s^2 S)]$  ions were measured by employing the ion-photon merged-beams technique at the Advanced Light Source synchrotron radiation facility. The energy ranges 197.5–200.5 eV, 201.9–202.1 eV of the  $[1s(2s\ 2p)^3 P]^2 P^o$  and  $[1s(2s\ 2p)^1 P]^2 P^o$  resonances, respectively, were investigated using resolving powers of up to 17 600. The energy range of the experiments was extended to about 238.2 eV yielding energies of the most prominent  $[1s(2\ell\ n\ell')]^2 P^o$  resonances with an absolute accuracy of the order of 130 ppm. The natural linewidths of the  $[1s(2s\ 2p)^3 P]^2 P^o$  and  $[1s(2s\ 2p)^1 P]^2 P^o$  resonances were measured to be  $4.8 \pm 0.6$  meV and  $29.7 \pm 2.5$  meV, respectively, which compare favourably with theoretical results of 4.40 meV and 30.53 meV determined using an intermediate coupling R-matrix method.

PACS numbers: 32.80.Fb, 31.15.Ar, 32.80.Hd, and 32.70.-n

Short title: K-shell photoionization of  $B^{2+}$  ions

Draft for J. Phys. B: At. Mol. & Opt. Phys: 15 June 2021

† Present address: Department of Physics, Jordan University of Science and Technology, Irbid, 22110, Jordan

‡ Corresponding author, E-mail: b.mclaughlin@qub.ac.uk

## 1. Introduction

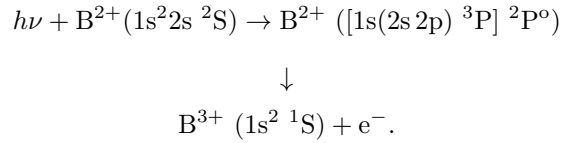
Satellites such as *Chandra* and *XMM-Newton* are currently providing a wealth of x-ray spectra on many astronomical objects. There is a serious lack of adequate atomic data, particularly in the K-shell energy range, needed for the interpretation of these spectra. Spectroscopy in the soft x-ray region (5–45 Å), including K-shell transitions for singly and multiply charged ionic forms of atomic elements such as; C, N, O, Ne, S and Si, and the L-shell transitions of Fe and Ni, provide a valuable probe of the extreme environments in active galactic nuclei (AGN's), x ray binary systems, and cataclysmic variables [1]. The goal of the present experimental and theoretical investigation is to provide accurate values for photoionization cross sections, resonance energies, and linewidths resulting from the photoabsorption of x rays near the K-edge of Li-like boron.

Previously, identification of Auger transitions from multiply charged ionic states of boron has been performed experimentally by using electron spectroscopy in ion-atom collisions [2, 3, 4], photon absorption and emission by laser-produced plasmas [5, 6], electron-impact ionization [7], beam-foil spectroscopy and high-resolution spark spectroscopy [8]. Theoretically resonance energies and linewidths for Auger transitions of the Li-like boron ion have been calculated using a variety of methods such as, perturbation theory in  $1/Z$  [9], B-splines [10] and the saddle-point method (SPM) with R-matrix or complex co-ordinate rotation methods [11, 12, 13]. A critical compilation of atomic transition probabilities for Be and B covering all stages of ionization (for allowed and forbidden outer-shell transitions) has recently been assembled [14]. To our knowledge this is the first time that measurements of the photoionization cross sections for the Li-like boron ion have been carried out for the photon energy range in the vicinity of the K-edge. To complement the high resolution measurements made at the Advanced Light Source (ALS) synchrotron radiation facility we have carried out photoionization cross section calculations using the R-matrix method. Recently, high resolution measurements for K-shell photoexcitation of singly, doubly and triply charged ions of carbon;  $C^+$  [15],  $C^{2+}$  [16] and  $C^{3+}$  [17] have been carried out within our international collaboration. A similar approach is used here to perform measurements on the doubly charged boron ion in the vicinity of the K-edge. Such studies are important in order to provide accurate results for absolute photoionization cross sections, resonance energies and natural linewidths. These benchmarked results therefore update existing literature values [18, 19, 20, 21] and as such should be used in preference to those that are currently in use in the various astrophysical modelling codes such as CLOUDY [22, 23] and XSTAR [24].

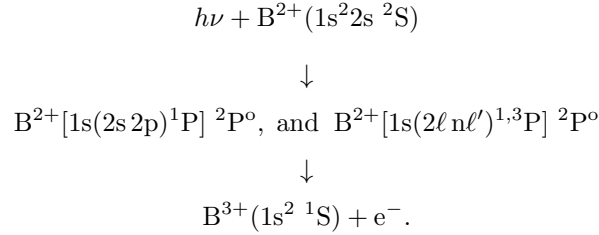
The present study aims to benchmark theoretical values for photoionization cross sections, resonance energies and lifetimes of autoionizing states of the  $B^{2+}$  ion in the vicinity of the K-edge with high-resolution experimental measurements. This provides confidence in the data that may be used in modelling astrophysical plasmas; e.g., in the hot (photoionized and collisionally ionized) gas surrounding  $\gamma$  Peg and  $\zeta$  Cas where B II and B III have been observed in absorption or for determining boron abundances in early B-type stars in the ORION association [25, 26].

Promotion in Li-like boron ( $B^{2+}$ ) ions of a K-shell electron to an outer np-valence shell ( $1s \rightarrow np$ ) from the ground state produces states that can autoionize, forming a  $B^{3+}$  ion and an outgoing free electron. The strongest excitation process in the interaction of a photon with the  $1s^2 2s^2 S$  ground-state of the Li-like boron ion is the

1s  $\rightarrow$  2p photo-excitation process;



At higher energies  $\text{B}^{2+}([1s(2s 2p)^1 \text{P}]^2 \text{P}^\circ)$  and  $\text{B}^{2+}([1s 2\ell n\ell']^2 \text{P}^\circ)$  states ( $n \geq 3$ ) are excited which subsequently decay primarily via autoionization processes;



The inner-shell autoionization resonances created (by the above processes) appear in the corresponding photoionization cross sections (in the energy region near to the K-edge) on top of a continuous background cross section for direct photoionization of the outer 2s electron. The present investigation provides absolute values (experimental and theoretical) for photoionization cross sections, resonance energies and linewidths for these states.

The layout of this paper is as follows. Section 2 presents a brief outline of the theoretical work. Section 3 details the experimental procedure used. Section 4 presents a discussion of the results obtained from both the experimental and theoretical methods. Finally in section 5 conclusions are drawn from the present investigation.

## 2. Theory

Theoretical cross-section calculations for the photoionization of doubly charged boron ions are available from the Opacity Project and can be retrieved from the TOPBASE database [27]. These cross-section calculations primarily cover the photon energy region corresponding to excitation of valence electrons and have been determined in *LS*-coupling. Theoretical results from the independent particle model exist in the energy region of the K-edge [19, 20, 21], but do not account for Auger states that have been observed, e.g., in the experimental studies of Rødbro and co-workers [2, 3, 4] or in the present study. Accurate theoretical estimates for the resonance energies and natural linewidths in the energy region of the K-edge for the  $\text{B}^{2+}$  ion have been provided previously by using the saddle-point method in combination with the R-matrix technique [12] and on the basis of the B-spline approach [10]. Agreement of that work was found for the energies of the  $[1s(2s 2p)^{1,3} \text{P}]^2 \text{P}^\circ$  resonance states with the previous experimental work of Rødbro and co-workers [4] and also with earlier theoretical work [9, 28, 29, 30, 31].

To benchmark theory for photoionization and obtain suitable agreement with high-resolution experimental photoionization measurements performed at third-generation synchrotron light source facilities (such as the ALS), state-of-the-art theoretical methods are required using highly correlated wavefunctions. Relativistic effects usually need to be included when the experimental resolution is such that

fine-structure effects can be resolved and radiation damping affects narrow resonances present in the photoionization cross sections. The features detailed above have been vividly illustrated in numerous experimental and theoretical photoionization studies within the present collaboration. Recent work on K-shell ionization of light ions involved He-like  $\text{Li}^+$  [32, 33], Li-like  $\text{C}^{3+}$  [17], Be-like  $\text{C}^{2+}$  [16], and B-like  $\text{C}^+$  [15].

Photoionization cross-section calculations for  $\text{B}^{2+}$  ions were performed both in  $LS$  and in intermediate coupling using the semi-relativistic Breit-Pauli approximation which allows for relativistic effects to be included. Radiation-damping [34] effects were also included for completeness within the confines of the R-matrix approach [35, 36]. An appropriate number of  $\text{B}^{3+}$  states (11  $LS$ , 17  $LSJ$  levels) were included in our intermediate coupling calculations. An  $n=4$  basis set of  $\text{B}^{3+}$  orbitals was used which was constructed using the atomic-structure code CIV3 [37] to represent the wavefunctions. Photoionization cross-section calculations were then performed in intermediate coupling for the  $1s^2 2s^2 S_{1/2}$  initial state of the  $\text{B}^{2+}$  ion. In the calculations the following eleven He-like  $LS$  states were retained:  $1s^2 \ ^1S$ ,  $1s ns \ ^{1,3}S$ ,  $1s np \ ^{1,3}P^\circ$ , and  $1s nd \ ^{1,3}D$ , for  $n \leq 3$ . The additional configurations  $1s np \ ^{1,3}P^\circ$ , and  $1s nd \ ^{1,3}D$ ,  $1s nf \ ^{1,3}F^\circ$ , ( $n = 4$ ), of the  $\text{B}^{3+}$  were used to account for correlation. This gives rise to 17  $LSJ$  states in the intermediate close-coupling expansions for the  $J=1/2$  initial scattering symmetry of the Li-like  $\text{B}^{2+}$  ion. For the structure calculations of the  $\text{B}^{3+}$  ion, all physical orbitals were included up to  $n=3$  in the configuration-interaction wavefunction expansions used to describe the states. The Hartree-Fock  $1s$  and  $2s$  tabulated orbitals of Clementi and Roetti [38] were used together with  $n=3$  orbitals which were determined by energy optimization on the appropriate spectroscopic state using the atomic structure code CIV3 [37]. The  $n=4$  correlation (pseudo) orbitals were determined by energy optimization on the  $1s 2s \ ^1S$  hole state of the  $\text{B}^{3+}$  ion in order to account for core relaxation and additional correlation effects in the multi-configuration interaction wavefunctions. All the states of the  $\text{B}^{3+}$  ion were then represented by using multi-configuration interaction wave functions. The Breit-Pauli  $R$ -matrix approach was used to calculate the energies of the  $\text{B}^{2+}(LSJ)$  states and the subsequent photoionization cross sections. A minor shift ( $< 0.1\%$ ) of the theoretical energies to experimental values was made so that they would be in agreement with available experimental thresholds [39]. Cross sections for photoionization out of the  $\text{B}^{2+}$  ( $1s^2 2s^2 S_{1/2}$ ) ground-state ion were then obtained for total angular momentum scattering symmetries of  $J = 1/2$  and  $J = 3/2$ , odd parity, that contribute to the total.

The  $R$ -Matrix method [35, 36, 34] was used to determine all the photoionization (PI) cross sections  $\sigma_{\text{PI}}(E)$ , for the initial ground state in intermediate-coupling ( $LSJ$ ). The scattering wavefunctions were generated by allowing all possible three-electron promotions out of the base  $1s^2 2s$  configuration of  $\text{B}^{2+}$  into the orbital set employed. Scattering calculations were performed with forty continuum functions and a boundary radius of 9.8 Bohr radii. For the  $^2S_{1/2}$  initial state the outer region electron-ion collision problem was solved (in the resonance region below and between all the thresholds) using a suitably chosen fine energy mesh of  $5 \times 10^{-8}$  Rydbergs ( $\approx 0.68 \mu\text{eV}$ ) to fully resolve all the extremely fine resonance structure in the photoionization cross sections. The multi-channel R-matrix QB technique (applicable to atomic and molecular complexes) of Berrington and co-workers [40, 41, 42] was used to determine the resonance parameters. The resonance width  $\Gamma$  was determined from the inverse of the energy derivative of the eigenphase sum  $\delta$  at the position of the resonance energy

$E_r$  via

$$\Gamma = 2 \left[ \frac{d\delta}{dE} \right]_{E=E_r}^{-1} = 2[\delta']_{E=E_r}^{-1} . \quad (1)$$

Averaging was performed over final total angular momentum  $J$  values. Finally, in order to compare directly with experiment, the theoretical cross section was convoluted with a Gaussian function of appropriate width to simulate the energy resolution of the measurements carried out at the Advanced Light Source synchrotron radiation facility.

### 3. Experiment

The experiment was performed at the ion-photon-beam (IPB) end-station of the undulator beamline 10.0.1 at the ALS. A detailed description of the experimental setup has been provided by Covington *et al* [43]. For the present study on  $B^{2+}$  similar procedures were utilized as in our earlier measurements on the K-shell photoionization cross sections for carbon ions [15, 16, 17]. Beams experiments with Li-like ions such as  $C^{3+}$  and  $B^{2+}$  are attractive since such ions can be provided almost exclusively in their ground state. The metastable  $^4P$  states of  $B^{2+}$  have lifetimes of less than 300 ns [44], much too short to survive the flight time of approximately 10  $\mu s$  from the ion source to the photon-ion interaction region.

The boron ions were generated from  $BF_3$  gas inside a compact all permanent-magnet electron cyclotron-resonance (ECR) ion source [45]. Collimated  $B^{2+}$  ion-beam currents of typically 30 nA were extracted by putting the ion source on a positive potential of +6 kV. After having travelled through a bending dipole magnet serving to select the desired ratio of charge to mass, the ion beam was centered onto the counterpropagating photon beam by applying appropriate voltages to several electrostatic ion beam steering devices. Downstream of the interaction region, the ion beam was deflected out of the photon beam direction by a second dipole magnet that also separated the ionized  $B^{3+}$  product ions from the  $B^{2+}$  parent ions. The  $B^{3+}$  ions were counted with nearly 100% efficiency with a single-particle detector, and the  $B^{2+}$  ion current was monitored for normalization. The measured  $B^{3+}$  count rate  $R$  was only partly due to photoionization events. It also contained  $B^{3+}$  ions produced by electron removal collisions with residual gas molecules and surfaces. This background was determined by mechanically chopping the photon beam.

Absolute cross sections were measured by normalizing the background-subtracted  $B^{3+}$  count rate to the measured ion current, to the photon flux, which was measured with a calibrated photodiode, and to the beam overlap. Beam overlap measurements were carried out using two commercial rotating-wire beam-profile monitors and a movable slit scanner. Absolute cross sections and resonance strengths for photoionization have thus been obtained with an estimated uncertainty of 20%. Detailed descriptions of the procedures for absolute measurements and of the budget of uncertainties have been provided previously by Covington *et al* [43]. Due to the considerable effort required for carrying out reliable absolute cross section measurements these were only performed at the peak positions of the dominant photoionization resonances.

Energy scan measurements were taken by stepping the photon energy through a preset range of values. The desired experimental energy spread was preselected by adjusting monochromator settings of the beamline accordingly. The scan

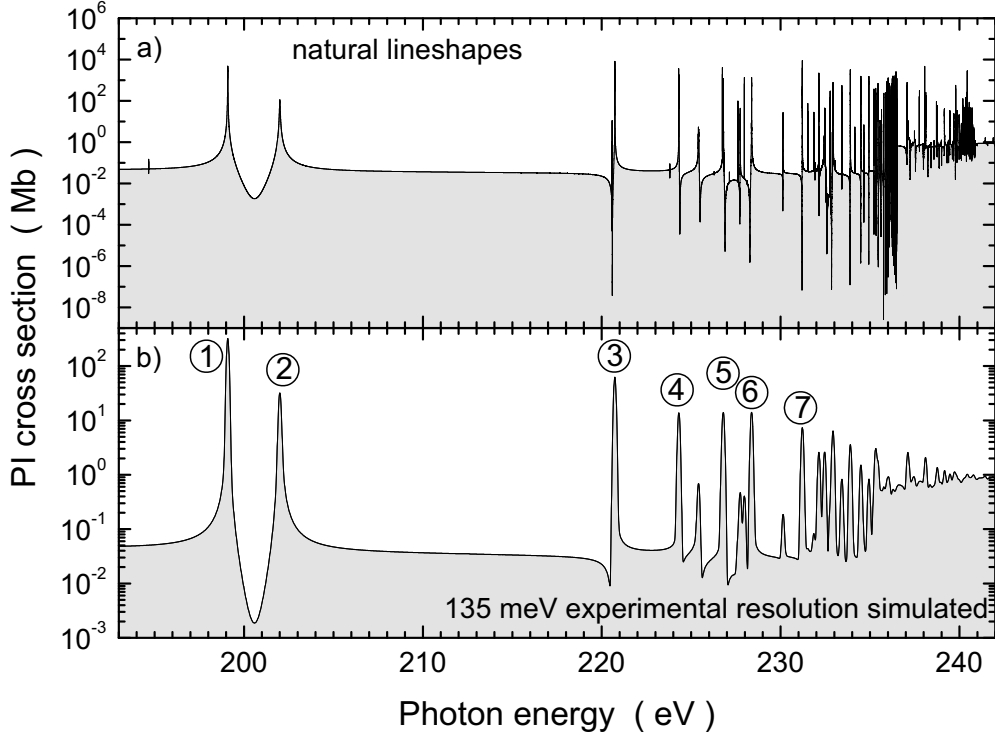


**Figure 1.** Theoretical cross sections for K-shell photoionization (PI) of Li-like  $B^{2+}$  from the 17-state intermediate-coupling R-matrix calculations; a) results showing the natural line shapes and interference of direct and resonant photoionization; b) the same calculations convoluted with a Gaussian distribution function of 135 meV full width at half maximum (FWHM). The K-edge at 236.496 eV is evident on the lower panel. Peaks ① through ⑦ observed in the experiment are designated respectively as;  $[1s(2s\ 2p)^3P]^2P^\circ$ ,  $[1s(2s\ 2p)^1P]^2P^\circ$ ,  $[(1s\ 2s\ ^3S)3p]^2P^\circ$ ,  $[(1s\ 2s\ ^1S)3p]^2P^\circ$ ,  $[(1s\ 2p\ ^1P)3s]^2P^\circ$ ,  $[(1s\ 2p\ ^1P)3d]^2P^\circ$  and  $[1s(3s\ 3p)^1P]^2P^\circ$ .

measurements were normalized to the absolute data points. The energy scale was calibrated by carrying out photoabsorption measurements with  $SF_6$  and Ar gas for the well known resonance features [46, 47] at energies 176–182 eV and 242–251 eV, respectively. Calibrated monochromator settings from these ranges were linearly interpolated to obtain the scaling factors for measured energies in the present range of interest. Since the parent ions are in motion, a Doppler correction has to be carried out transforming the nominal laboratory energies to the center-of-mass frame of the ions before applying the calibration factor. With all this carefully included, we estimate an uncertainty of at most  $\pm 30$  meV for the energy scale of the present measurements. Since the precision of peak position determinations is of the order of better than 1 meV, the possible calibration error almost exclusively determines the absolute uncertainties of the resonance energies.

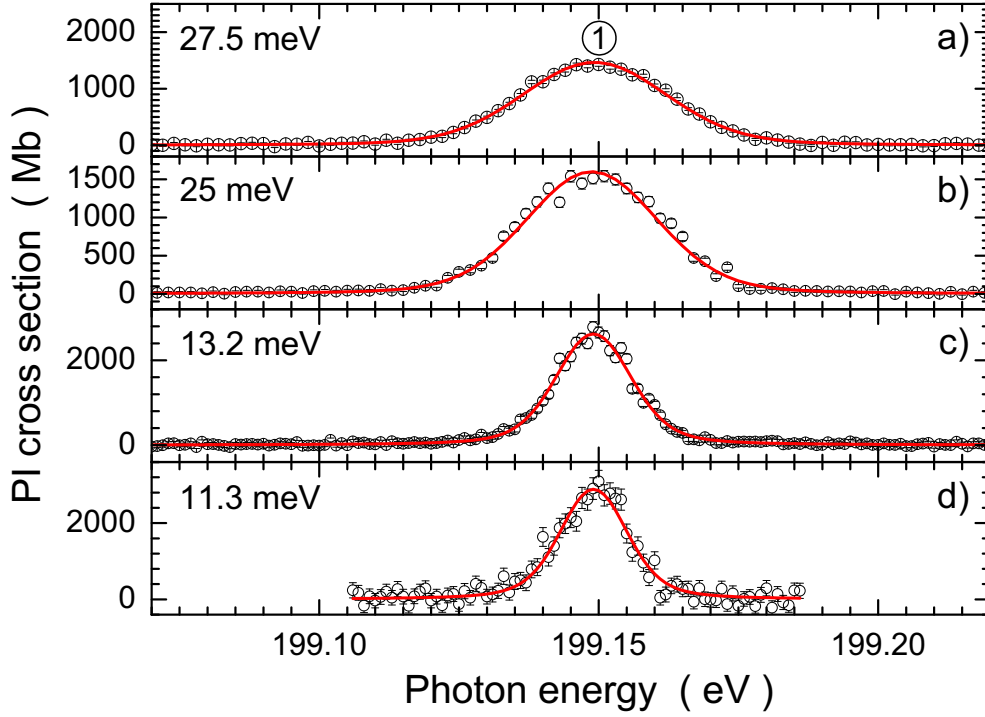


**Figure 2.** (Colour online) Series of energy scans taken for peak ① in figure 1. The scan cross sections were normalized to an absolute measurement at the peak energy so that all data sets are on an absolute scale. The peak is associated with the  $[1s(2s2p)^3P]^2P^\circ$  resonance in  $B^{2+}$  ions. The experimental energy spreads given for each individual measurement were determined by Voigt fits (red solid lines) to the experimental data.

#### 4. Results and Discussion

Figure 1 shows the theoretical photoionization cross section spectra for the  $B^{2+}$  ion obtained from our intermediate-coupling R-matrix results in the photon energy range 193–242 eV. In figure 1 a) the theoretical results are displayed in their natural form. For the graph in figure 1 b) the theoretical results were convoluted with a Gaussian distribution function of 135 meV full width at half maximum. The resonance peaks labelled ① through ⑦ shown in the convoluted theoretical photoionization spectrum of figure 1 b) have been observed in the photoionization experimental data taken at the ALS. On the logarithmic scale of this figure, one can clearly observe interference features resulting from the interaction of direct 2s photoionization and K-shell excitation resonances. The resulting changes at the level of the 2s ionization continuum are so small, however, that they are not accessible to the present experiment.

The experimental and theoretical results for K-shell photoionization cross sections of the  $B^{2+}$  ion are shown in figures 2–5. The solid black lines in figures 4 and 5 are the theoretical results from the R-matrix calculations including radiation damping and convoluted with a Gaussian of the appropriate experimental resolution. The results

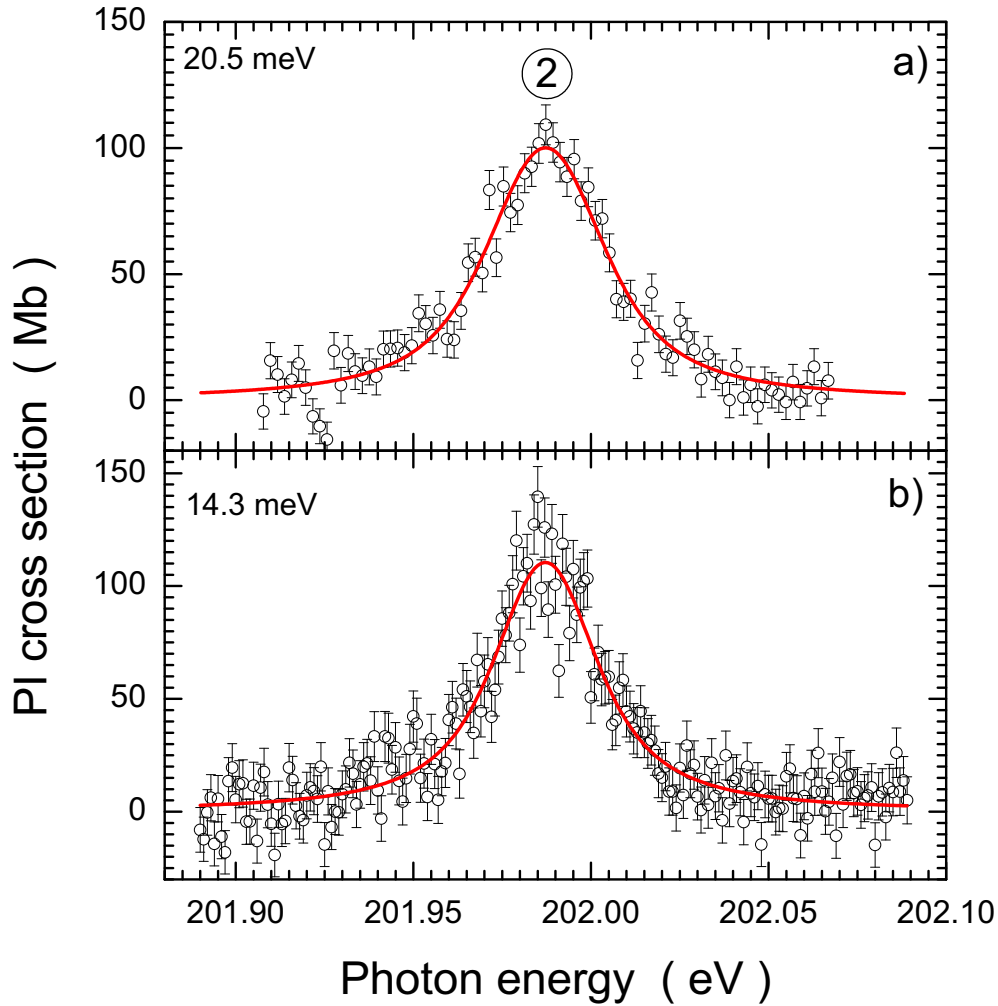


**Figure 3.** (Colour online) Energy scans taken for peak ② in figure 1. Like the data in figure 2 the cross sections are on an absolute scale with statistical error bars provided. The peak is associated with the  $[1s(2s2p)^1P]^2P^o$  resonance in  $B^{2+}$  ions. The experimental energy spreads were determined by Voigt fits (red solid lines) to the experimental data.

from the ALS experiment in figures 2 – 5 are indicated by the open circles (diamonds instead of open circles in figure 5 to indicate the greatly different experimental energy spread in that particular measurement) and the solid red lines (dotted red lines in figures 4 and 5) represent Voigt fits to the data. From the Voigt fits to the experimental data experimental energy spreads were determined. These energy spreads are given in figures 2 and 3 in each panel. For figure 4 they are 27.5 meV for peak ①, 20.5 meV for peak ②, 25.5 meV for peak ③, 26 meV for peak ④, 22.6 meV for peak ⑤, and 25.4 meV for peak ⑥. In figure 5 a scan measurement with 135 meV energy spread is shown. The inset shows peak ⑦ again but this time measured with an experimental energy spread of 26.3 meV.



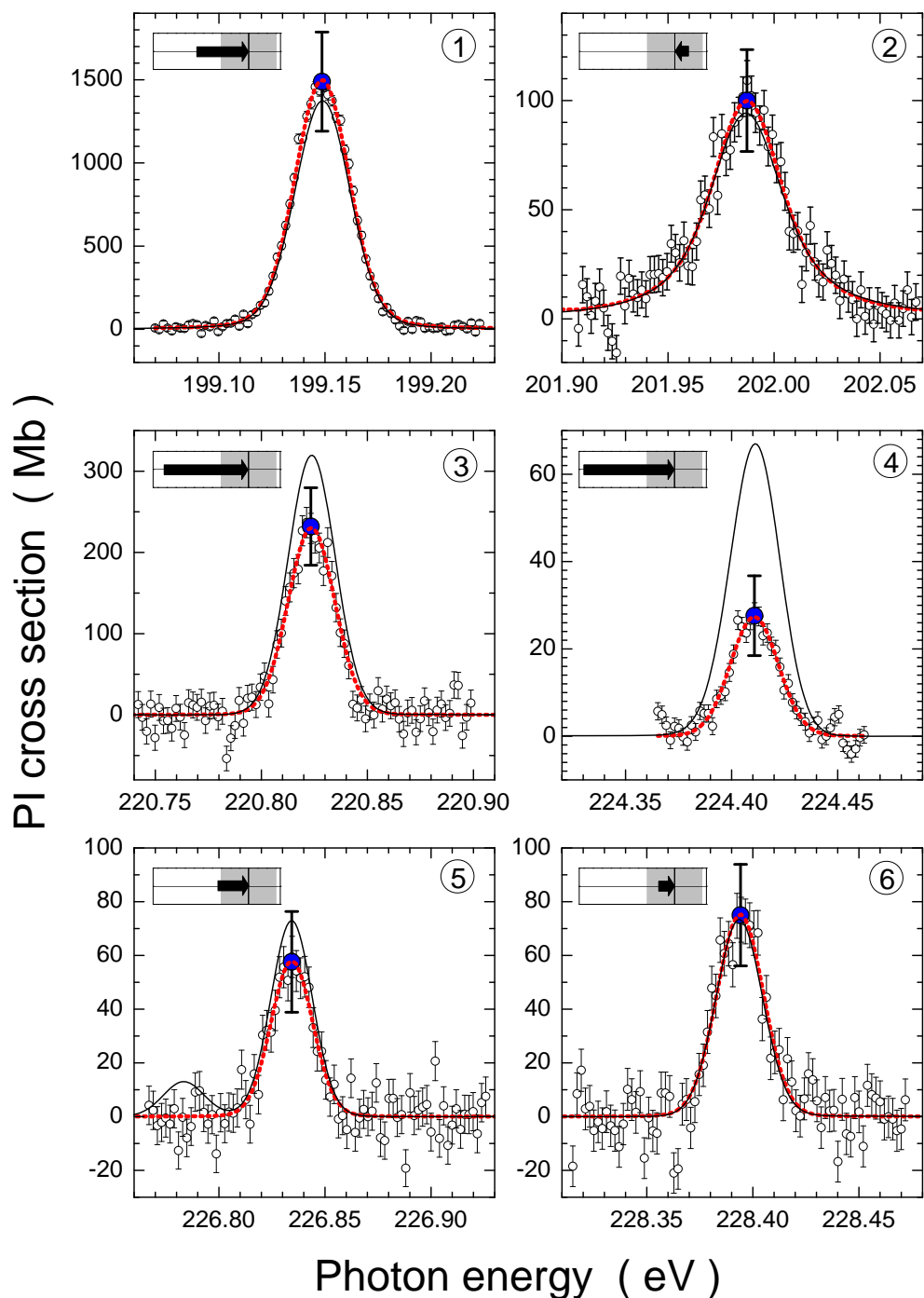


**Figure 4.** (Colour online) Energy scan measurements taken for peaks ① through ⑥ in figure 1. The scan cross sections are shown with statistical uncertainties. The data were normalized to absolute measurements at the peak energy (shown as blue shaded circles with fat error bars). Voigt fits to the experimental data are represented by the (red) dotted lines. The R-matrix results were convoluted with Gaussians of appropriate widths for each individual peak. The theory curves (solid black lines) were then shifted to the measured peak positions. The shifts necessary to match theory with experiment are visualized by the lengths of the arrows inside the boxes in the upper left corner of each panel. Each box represents an energy range from  $-105$  meV to  $+35$  meV around the resonance energy. The gray shaded area represents an experimental uncertainty range of  $\pm 30$  meV. An arrow from left to right indicates that the calculated resonance had to be shifted to higher energies.

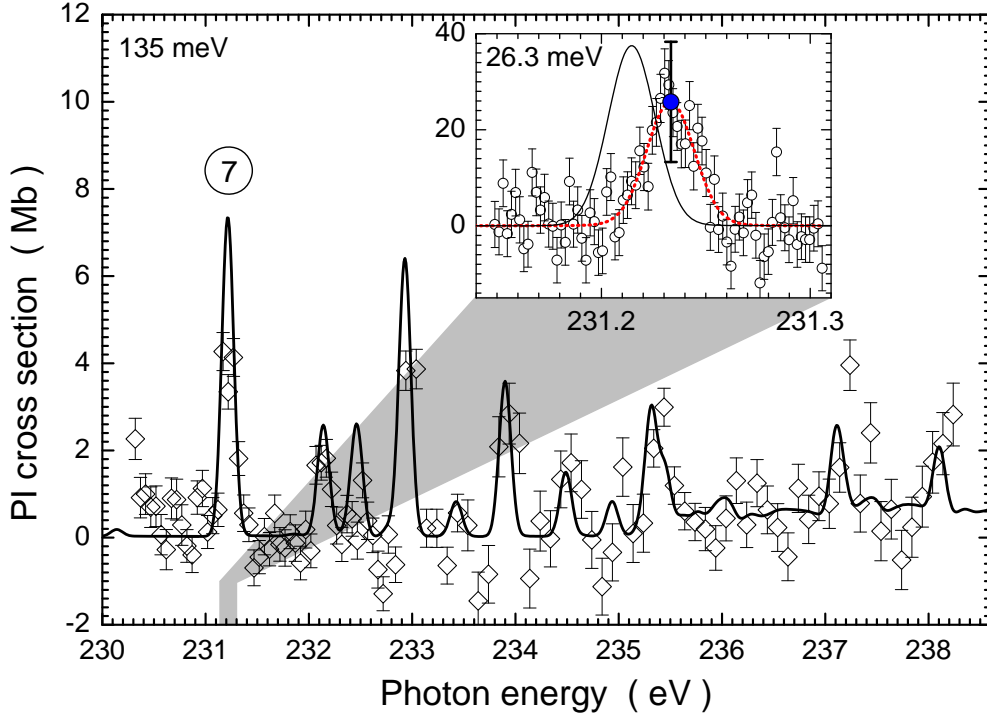


**Figure 5.** (Colour online) Energy scan measurement taken in the energy range from 230.3–238.3 eV at an experimental energy spread of 135 meV. The open diamonds with their statistical error bars were obtained by averaging over 5 adjacent measurements. The scan cross sections were normalized to the absolute measurement at the centre of peak ⑦ (shown as blue shaded circle with fat error bars in the inset) so that the data are on an absolute scale. Peak ⑦ was separately scanned at a resolution of 26.3 meV (see inset) determined by a Voigt fit (red dotted line) to the experimental data. The R-matrix results from the lower panel of figure 1 are displayed as a solid black line. The inset also shows the R-matrix results as a non-shifted solid black line that was obtained by convolution with a Gaussian of 26.3 meV FWHM. The energy range of the inset is 170 meV, i.e., the same as in all panels of figure 4. The shading indicates the origin of the inset panel on the energy axis of the present graph.

Figures 2 and 3 show the ALS experimental data for the  $B^{2+}$  ion in the energy region of the first two resonance peaks (the  $[1s(2s2p)^{1,3}P]^2P^o$  resonances) taken during the course of the measurements with varying degrees of resolution. By fitting Voigt profiles to the different sets of peak measurements the experimental energy spreads, the natural resonance widths and resonance energies can be determined. Each single scan of a resonance can contribute to the accuracy of the resonance parameters obtained. The lowest-energy-spread experiments are especially valuable for the determination of the natural line width. The measurement with the smallest energy spread may, however, suffer from statistics and thus a higher-energy-spread experiment with better statistics may add significantly to the accurate determination of the natural resonance width and resonance energy. Thus for peak ① we obtained widths  $\Gamma = 4.5 \pm 1.7$  meV from the experimental data shown in figure 2 panel d) at the highest resolution and  $\Gamma = 5.2 \pm 0.5$  meV from the experimental data shown in figure 2 panel c). The data

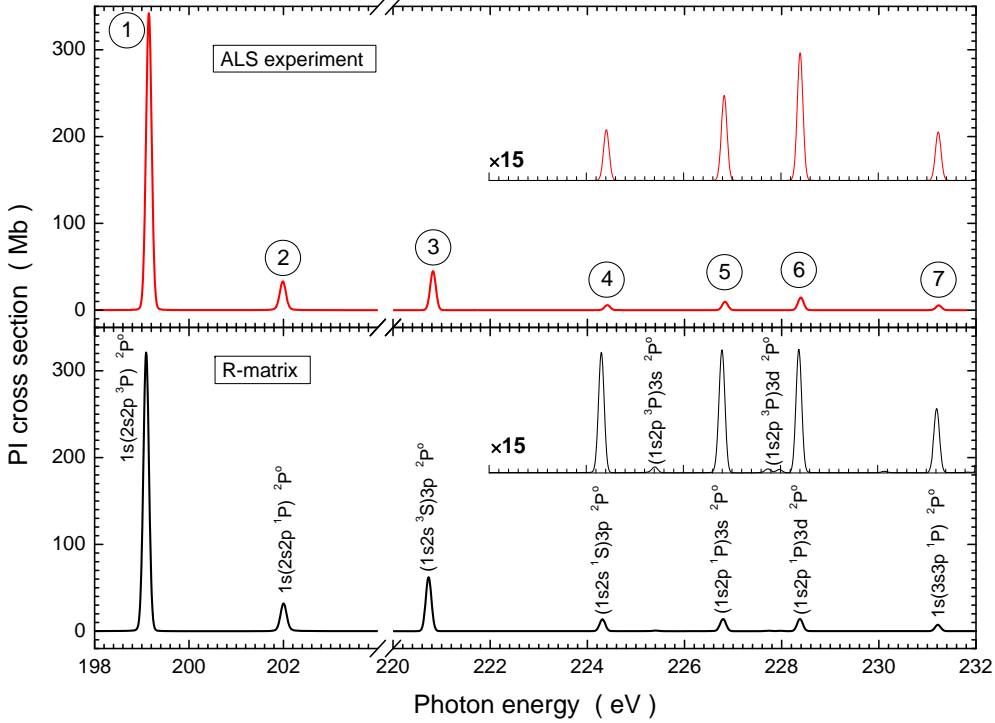


**Figure 6.** (Colour online) Comparison of theory and experiment in an overview. The lower panel shows the theory data taken from the lower panel of figure 1 now displayed on a linear scale. The suggested peak assignments are provided. The cross sections in the energy range above 222 eV were multiplied by a factor of 15 and displayed with an offset. The red line in the upper panel is based on fits to the experimental results of this study: the Voigt profiles of resonances no. 1 through 7 were simulated for an experimental energy spread of 135 meV using the information obtained from the Voigt fits to the experimental data displayed in figures 2 – 5.

from figure 2 panels a) and b) where inconclusive with respect to the line width when fitted individually. Similarly, for peak ② we obtained widths  $\Gamma = 29.5 \pm 3.3$  meV from the experimental data shown in figure 3 panel b) and  $\Gamma = 30.2 \pm 3.9$  meV from the experimental data shown in figure 3 panel a).

Clearly, the result obtained from several independent measurements can be expected to be of better quality than the results of each single measurement. Therefore, by combining all data sets obtained for a specific resonance in a multiple-peak fit one can improve the accuracy of the final result. In such a least squares multiple-peak fit all measurements are considered in a single fit procedure. The resonance energy  $E_{\text{ph}}^{(\text{res})}$  and the natural width  $\Gamma$  of the resonance investigated in several individual measurements are varied in order to minimize the sum of all squared deviations in all measurements at a time. Of course, they have to be kept the same for all the different individual peak measurements on one specific resonance. Fitting the 4 measurements of peak ① shown in figure 2 in one least-squares fit session provides  $\Gamma = 4.8 \pm 0.6$  meV. Similarly, a combined fit of the 2 measurements of peak ② in figure 3 yields  $\Gamma = 29.7 \pm 2.5$  meV. While the fit results obtained for the first

two peaks are of very satisfying quality, Fano parameters describing the interference of direct and resonant photoionization channels were not accessible to the present experiment. The results that could be obtained from these nonlinear least-squares fits to the measured data illustrated in figures 2 and 3 are presented in table 1. Apart from the resonance energies  $E_{\text{ph}}^{(\text{res})}$  and the Lorentzian widths  $\Gamma$ , experimental resonance strengths  $\bar{\sigma}^{\text{PI}}$  were also obtained which result from integration of the cross section  $\sigma_{\text{PI}}(\text{E}; L_i S_i \rightarrow L_j S_j)$  for a specific resonance transition over all energies

$$\bar{\sigma}^{\text{PI}} = \int_E \sigma_{\text{PI}}(\text{E}; L_i S_i \rightarrow L_j S_j) d\text{E} \quad . \quad (2)$$

Table 1 displays the corresponding ALS experimental results together with the present  $LS$  and intermediate-coupling R-matrix calculations in addition to those from the earlier experimental [4, 5, 6, 8, 11] and theoretical [10, 12, 13, 31] studies. Comparisons of the resonance parameters (see table 1) for the  $[1s(2s2p)^3P]^2P^\circ$  (peak ①) and  $[1s(2s2p)^1P]^2P^\circ$  (peak ②) resonances determined experimentally with the current and previous theoretical estimates show a very satisfying level of agreement. The uncertainties of the experimental data for the excitation energies  $E_{\text{ph}}^{(\text{res})}$  are limited by the existing calibration standards in the case of the present work and the previous study by Kennedy *et al* [5] with error bars of 30 meV. The electron spectroscopy data have uncertainties of 100 meV, considerably higher than the photon experiments. The data provided by Kramida *et al* [8] have the character of recommended data and as such are based not only on existing experiments but also on theoretical calculations using *ab initio* and semi-empirical techniques. The estimated uncertainties are only 10 meV and 14 meV for the energies of the  $[1s(2s2p)^3P]^2P^\circ$  and  $[1s(2s2p)^1P]^2P^\circ$  resonances, respectively. The present experiment is closest to this work for both peaks ① and ②.

All experimental  $E_{\text{ph}}^{(\text{res})}$  results for peak ① agree with one another within their uncertainties. The present R-matrix result is within about 50 meV from the most accurate experimental data. The theoretical data closest to experiment are those resulting from the configuration interaction expansion calculations using a B-spline basis set [10]. The result of the saddle-point method with R-matrix calculations [12] has the largest discrepancy with respect to the photoexcitation experiments with a deviation of 130 meV from the present experimental result and 149 meV from the excitation energy recommended by Kramida *et al* [8]. For peak ② the experiment by Kennedy *et al* [5] is outside the uncertainty ranges of the other photoexcitation experiments with a difference of about 100 meV to the present experimental results. The scatter of the theory data is similar to that observed for peak ①. The agreement of the present  $LSJ$  R-matrix calculation for peak ② with the present experiment is perfect while the B-spline method is 37 meV above the present experiment and 48 meV above the energy recommended by Kramida *et al* [8]. It is interesting to note that the differences of resonance energies obtained for peaks ① and ② by theory and experiment show a considerably reduced scatter range, about one third, as compared to the resonance energies themselves. Excellent agreement with respect to the energy splitting is found for the present experiment with  $2.838 \pm 0.001$  meV, the photoexcitation experiment by Jannitti *et al* [6] (8 meV lower) and the data of Kramida *et al* [8] (8 meV higher). With respect to these experimental data the theoretical predictions on the average are 50 meV too high.

In the prediction of the Lorentzian width of peak ① the different theoretical approaches, all within the span of different versions of the saddle-point method, cover

**Table 1.** Comparison of photoionization resonance energies  $E_{\text{ph}}^{(\text{res})}$  (in eV), natural linewidths  $\Gamma$  (meV) and resonance strengths  $\bar{\sigma}^{\text{PI}}$  (in Mb eV) for  $\text{B}^{2+}$  ions from our present ALS experimental work and R-matrix theoretical (11-state  $LS$ -coupling and 17-state intermediate coupling) calculations with previous studies for peaks ① and ②. For the conversion of the wavelength scale of some of the previous work to the present energy scale  $hc = 1239.841\,875$  eV nm has been used. For the conversion of  $\text{B}^{2+}$  Auger energies obtained by Chung and Bruch [11] to the  $\text{B}^{2+}$  excitation energies in the present table the ionization potential of 37.9306 eV for  $\text{B}^{2+}$  ions as tabulated by Ralchenko *et al* [39] was added.

Resonance (Label)		ALS/Others (Experiment)	R-matrix (Theory)	SPM/B-spline (Theory)
[1s(2s 2p) <sup>3</sup> P] <sup>2</sup> P <sup>o</sup> ①	$E_{\text{ph}}^{(\text{res})}$	199.149 ± 0.030 <sup>†</sup>	199.092 <sup>a</sup>	199.279 <sup>c</sup>
		199.130 ± 0.010 <sup>f</sup>	199.081 <sup>b</sup>	199.101 <sup>d</sup>
		199.17 ± 0.03 <sup>g</sup>		199.145 <sup>e</sup>
		199.17 ± 0.1 <sup>h</sup>		199.181 <sup>l</sup>
		199.20 <sup>k</sup>		
	$\Gamma$	4.8 ± 0.6 <sup>†</sup>	4.40 <sup>a</sup>	5.27 <sup>c</sup>
			4.45 <sup>b</sup>	4.00 <sup>d</sup>
				4.29 <sup>e</sup>
				4.05 <sup>l</sup>
	$\bar{\sigma}^{\text{PI}}$	51 ± 10 <sup>†</sup>	45.34 <sup>a</sup>	
		45.66 <sup>b</sup>		
[1s(2s 2p) <sup>1</sup> P] <sup>2</sup> P <sup>o</sup> ②	$E_{\text{ph}}^{(\text{res})}$	201.987 ± 0.030 <sup>†</sup>	201.991 <sup>a</sup>	202.227 <sup>c</sup>
		201.976 ± 0.014 <sup>f</sup>	201.941 <sup>b</sup>	201.987 <sup>d</sup>
		202.03 <sup>k</sup>		202.024 <sup>e</sup>
		202.05 ± 0.1 <sup>h</sup>		202.041 <sup>l</sup>
		202.09 ± 0.03 <sup>g</sup>		
	$\Gamma$	29.7 ± 2.5 <sup>†</sup>	30.53 <sup>a</sup>	29.83 <sup>c</sup>
			30.34 <sup>b</sup>	29.80 <sup>d</sup>
				30.52 <sup>e</sup>
				30.60 <sup>l</sup>
	$\bar{\sigma}^{\text{PI}}$	5.7 ± 1.2 <sup>†</sup>	5.16 <sup>a</sup>	
		5.37 <sup>b</sup>		

<sup>†</sup>Present ALS experimental results

<sup>a</sup>Breit-Pauli semi-relativistic intermediate coupling R-matrix (17-state).

<sup>b</sup>Non-relativistic  $LS$  coupling R-matrix (11-state).

<sup>c</sup>Saddle-point method (SPM) with R-matrix [12].

<sup>d</sup>Saddle-point method (SPM) with Complex Rotation [13]

<sup>e</sup>B-spline method [10]

<sup>f</sup>Beam-foil spectroscopy and high-resolution spark spectroscopy [8]

<sup>g</sup>Laser-produced plasmas experiment [5]

<sup>h</sup>Electron spectroscopy experimental data [4] revised [11]; the error bars of 0.1 eV are the estimates from the work of Chung and Bruch [11] who provide the Auger energies with 5-digit numbers

<sup>k</sup>Laser-produced plasmas experiment, no uncertainties specified [6]

<sup>l</sup>Saddle-point method (SPM) with relativistic corrections [31]

**Table 2.** Resonance energies  $E_{\text{ph}}^{(\text{res})}$  (in eV), natural linewidths  $\Gamma$  (meV) and resonance strengths  $\bar{\sigma}^{\text{PI}}$  (in Mb eV) for  $\text{B}^{2+}$  ions from our present experimental (ALS) and theoretical (R-matrix) work compared with previous studies for the higher lying resonances (peaks ③ through ⑦) in the energy range 220–232 eV. For conversions from different energy scales of other original work to the present excitation energies see table 1.

Resonance (Label)		ALS/Others (Experiment)	R-matrix (Theory)	B-spline/SPM (Theory)
[(1s 2s $^3\text{S}$ )3p] $^2\text{P}^{\circ}$ ③	$E_{\text{ph}}^{(\text{res})}$	220.823 $\pm$ 0.030 <sup>†</sup>	220.721 <sup>a</sup>	220.826 <sup>b</sup>
		220.73 <sup>c,*</sup>		220.851 <sup>g</sup>
		220.766 $\pm$ 0.074 <sup>d</sup>		
		220.77 $\pm$ 0.08 <sup>e,*</sup>		
		220.80 $\pm$ 0.2 <sup>f</sup>		
	$\Gamma$		0.50 <sup>a</sup>	0.46 <sup>b</sup>
	$\bar{\sigma}^{\text{PI}}$	6.5 $\pm$ 1.3 <sup>†</sup>	8.99 <sup>a</sup>	0.38 <sup>g</sup>
[(1s 2s $^1\text{S}$ )3p] $^2\text{P}^{\circ}$ ④	$E_{\text{ph}}^{(\text{res})}$	224.411 $\pm$ 0.030 <sup>†</sup>	224.301 <sup>a</sup>	224.416 <sup>b</sup>
		224.20 <sup>c</sup>		224.476 <sup>g</sup>
		224.37 $\pm$ 0.08 <sup>e</sup>		
		224.374 $\pm$ 0.037 <sup>d</sup>		
		224.41 $\pm$ 0.2 <sup>f</sup>		
	$\Gamma$		0.28 <sup>a</sup>	0.26 <sup>b</sup>
	$\bar{\sigma}^{\text{PI}}$	0.79 $\pm$ 0.2 <sup>†</sup>	1.88 <sup>a</sup>	
[(1s 2p $^3\text{P}$ )3s] $^2\text{P}^{\circ}$	$E_{\text{ph}}^{(\text{res})}$		225.407 <sup>a</sup>	225.482 <sup>b</sup>
		225.416 $\pm$ 0.005 <sup>d</sup>		225.554 <sup>g</sup>
		225.44 $\pm$ 0.2 <sup>f</sup>		
	$\Gamma$		11.39 <sup>a</sup>	11.39 <sup>b</sup>
				11.32 <sup>g</sup>
[(1s 2p $^1\text{P}$ )3s] $^2\text{P}^{\circ}$ ⑤	$E_{\text{ph}}^{(\text{res})}$	226.834 $\pm$ 0.030 <sup>†</sup>	226.791 <sup>a</sup>	226.849 <sup>b</sup>
		226.680 $\pm$ 0.037 <sup>d</sup>		
			0.46 <sup>a</sup>	0.47 <sup>b</sup>
	$\Gamma$		1.80 <sup>a</sup>	
	$\bar{\sigma}^{\text{PI}}$	1.5 $\pm$ 0.3 <sup>†</sup>		
[(1s 2p $^3\text{P}$ )3d] $^2\text{P}^{\circ}$	$E_{\text{ph}}^{(\text{res})}$		227.731 <sup>a</sup>	227.760 <sup>b</sup>
	$\Gamma$		0.59 <sup>a</sup>	0.46 <sup>b</sup>
[(1s 2p $^1\text{P}$ )3d] $^2\text{P}^{\circ}$ ⑥	$E_{\text{ph}}^{(\text{res})}$	228.394 $\pm$ 0.030 <sup>†</sup>	228.371 <sup>a</sup>	
	$\Gamma$		0.66 <sup>a</sup>	
	$\bar{\sigma}^{\text{PI}}$	2.1 $\pm$ 0.6 <sup>†</sup>	2.03 <sup>a</sup>	
[1s(3s 3p) $^1\text{P}$ ] $^2\text{P}^{\circ}$ ⑦	$E_{\text{ph}}^{(\text{res})}$	231.233 $\pm$ 0.030 <sup>†</sup>	231.201 <sup>a</sup>	
	$\Gamma$		0.07 <sup>a</sup>	
	$\bar{\sigma}^{\text{PI}}$	0.8 $\pm$ 0.3 <sup>†</sup>	1.07 <sup>a</sup>	

<sup>†</sup>Present ALS experimental results.

<sup>a</sup>Breit-Pauli semi-relativistic intermediate coupling R-matrix (17-state).

<sup>b</sup>B-spline method [10]

<sup>c</sup>Laser-produced plasmas experiment, no uncertainties specified [6]

<sup>d</sup>Beam-foil spectroscopy and high-resolution spark spectroscopy [8]

<sup>e</sup>Laser-produced plasmas experiment [5]

<sup>f</sup>Electron spectroscopy experimental data [4] revised [11]; the error bars of 0.2 eV are the estimates from the work of Chung and Bruch [11] who provide the Auger energies with 5-digit numbers

<sup>g</sup>Saddle-point method (SPM) with relativistic corrections [31]

\*Line assignment changed as suggested by Kramida *et al* [8]

a range from 4.0 meV to almost 5.5 meV, i.e., they differ by up to about 30% from the lowest width calculated. The present R-matrix calculations agree best with the experiment but also the saddle-point method with R-matrix [12] calculations and the B-spline method [10] are within the present experimental error bars. For peak ② with its larger width all theoretical data and the present experiment are in very good accord. Since this is the first time that Lorentzian widths of core-excited states of the  $B^{2+}$  ion have been experimentally determined, there are no other measurements to compare with. In general, discrimination of specific theoretical approaches is not easily possible on the basis of the existing experimental data for  $E_{\text{ph}}^{(res)}$  and  $\Gamma$  provided in table 1. In view of all available data, both theoretical and experimental, the excitation energies from the saddle-point method with R-matrix calculations [12] appear to be too high (at a level of 0.1 eV).

From the experimental resonance strengths also the oscillator strengths  $f$  may be determined using the relationship,

$$f(L_i S_i \rightarrow L_j S_j) = \frac{\bar{\sigma}^{\text{PI}}}{4\pi^2 \alpha a_0^2 \mathcal{R}} \quad , \quad (3)$$

with the fine structure constant  $\alpha$ , the first Bohr radius  $a_0$  and the Rydberg energy  $\mathcal{R}$ . For the two resonances in table 1, the oscillator strengths obtained from the experimental results yield values of  $0.46 \pm 0.09$  for the first resonance at 199.149 eV and  $0.052 \pm 0.010$  for the second resonance at 201.987 eV which are in suitable agreement with our theoretical estimates of 0.41 ( $LSJ$ ), 0.42 ( $LS$ ) and 0.047 ( $LSJ$ ), 0.049 ( $LS$ ). We note that any tiny contributions to the decay rate from radiative processes are negligible compared to our absolute error bars. Thus the measured photoionization resonances account for almost all of the oscillator strength in these transitions.

Table 2 gives the values determined for the resonance energies and resonance strength parameters of the remaining higher lying resonances located in the energy region 220–238.3 eV along with the corresponding theoretical values. From table 2 (due to the limited scan ranges and the resolution of the individual scans around 25 meV applied in the region 220–230 eV) it is seen that we were not able to resolve and detect the two small resonances (i.e. the peak lying between ④ and ⑤, and that between ⑤ and ⑥) in the spectra for this energy range. For the peaks that we have been able to observe experimentally (and determine their resonance parameters and tentatively designate), a comparison with theory shows the results are in suitable agreement both with our theoretical estimates and those from earlier studies.

The Lorentzian widths of the resonances discussed in table 2 could not be experimentally determined. Most of the states have calculated widths between 0.07 meV and 0.66 meV, a range that is presently not experimentally accessible. Only the  $[(1s2p\ ^3P)3s]^2P^o$  resonance is predicted theoretically to have a width of 11.4 meV, sufficiently broad for the possible energy resolution of the experimental arrangement. However, this resonance is so small it could not even be detected in the measurements. Where a comparison is possible the Lorentzian widths resulting from the present R-matrix approach agree very well with the results of the B-spline method [10] and saddle-point method with relativistic corrections [11]. Discrepancies are typically within less than 10%.

The experimental resonance energies given in table 2 for peak ③ (assigned to the excited  $[(1s2s\ ^3S)3p]^2P^o$  state) are all within their mutual error bars. The scatter of the theoretical data is not more than 130 meV. For peak ④ (assigned to the excited  $[(1s2s\ ^1S)3p]^2P^o$  state) the experimental results apart from that by Jannitti *et al* [6]

(no error bars quoted, difference about 0.2 eV) agree very well with one another. The theory data are close to the experiments that quote the lowest uncertainties. For peaks ③ through ⑦ the present experimental results for the resonance energies have the smallest uncertainty with a conservative estimate of  $\pm 30$  meV. For the  $[(1s 2p^3 P) 3s]^2 P^\circ$  resonance, not seen in the present experiment, Kramida *et al* [8] estimated an uncertainty of only 5 meV of their resonance energy. This is barely in agreement with the present R-matrix results and would rule out the results from the B-spline method [10] and saddle-point method with relativistic corrections [11] which differ by 66 meV and 139 meV, respectively.

For peak ⑤ (assigned to the excited  $[(1s 2p^1 P) 3s]^2 P^\circ$  state) the present resonance energy and that of Kramida *et al* [8] differ by 154 meV, far outside the mutual error bars. On the other hand the available theoretical calculations agree with the present experiment within its error bar. Given the excellent agreement of the present energies and the data of Kramida *et al* [8] in all other cases one must assume a misprint in their table or a problem with the assignment of the state associated with the quoted energy. For the  $[(1s 2p^3 P) 3d]^2 P^\circ$  resonance not seen in the present experiment, the present R-matrix resonance energy is within 31 meV from the result of the B-spline method [10]. For the remaining peaks ⑥ and ⑦ (assigned to the excited  $[(1s 2p^1 P) 3d]^2 P^\circ$  and  $[1s(3s 3p)^1 P]^2 P^\circ$  states, respectively) there are no data other than the present theory and experiment. They are compared with one another in the context of figures 4 and 5. Overall, the level-energy results of the B-spline method [10], where available, are found to be the theoretical data closest to the most accurate experiments.

The theoretical data in figure 4 (for peaks ① through ⑥) was shifted by minor amounts (details are given in the caption) to match the experimental data. In order to make a direct comparison with the absolute experimental data, the theoretical cross sections were convoluted with Gaussians of the appropriate widths. In figure 5 we show the comparison between theory and experiment in the energy range 230.0–238.3 eV, where the theoretical data has been convoluted with a Gaussian of 135 meV FWHM. Finally, figure 6 illustrates the comparison between the present R-matrix intermediate coupling calculations and the ALS experimental results over the energy range incorporating the 7 peaks observed in the experiment. The spectral overview in figure 6 illustrates a simulated ALS spectrum expected on the basis of the resonance parameters from the present measurements and their analysis assuming the cross sections were all measured with 135 meV resolution (the experimental spectrum displayed in figure 5 was indeed measured at 135 meV resolution). As can be seen from figure 6 over the complete energy region studied excellent agreement is observed between the present theoretical R-matrix calculations performed in intermediate coupling and the experimental data taken at the ALS. The figure also indicates the resonances that were not observed in the experiments because of their small cross sections.

## 5. Conclusion

Photoionization of  $B^{2+}$  ions was studied both experimentally and theoretically in the energy region of the K-edge. Overall, excellent agreement is found between the present theoretical and experimental results both on the photon-energy scale and on the absolute photoionization cross-section scale for this prototype Li-like system for the majority of the observed peaks. Minor discrepancies however do exist between theory and experiment (when the energy range around narrow resonances is strongly



expanded) both for resonance strengths and positions. This may be possibly attributed to the limitations of the  $n=4$  basis set used in the present theoretical work.

The strength of the present study is in its excellent experimental resolving power coupled with theoretical predictions using the Breit-Pauli R-matrix method. The experimental energy resolution of 11.3 meV and 14.3 meV for the first two peaks in the present work made possible the determination of the linewidths of the  $[1s(2s2p)^{1,3}P]^2P^o$  resonances. The Voigt line-profile fit (to the ALS experimental data) for these two resonances yielded values respectively (see table 1) for the linewidth of  $4.8 \pm 0.6$  meV and  $29.7 \pm 2.5$  meV which are in good agreement with the present R-matrix theoretical predictions of 4.40 meV and 30.53 meV (5.27 meV and 29.53 meV from the saddle-point-method with R-matrix [12] and 4.0 meV and 29.8 meV from the saddle-point-method with complex co-ordinate rotation [13]). Our linewidth results are also in excellent accord with the values of 4.29 meV and 30.52 meV from the B-spline method [10] for these same two resonances.

### Acknowledgments

We acknowledge support by Deutsche Forschungsgemeinschaft under project number Mu 1068/10 and through NATO Collaborative Linkage grant 976362 as well as by the US Department of Energy (DOE) under contract DE-AC03-76SF-00098 and grant DE-FG02-03ER15424. B M McLaughlin acknowledges support by the US National Science Foundation through a grant to ITAMP at the Harvard-Smithsonian Center for Astrophysics. The computational work was carried out at the National Energy Research Scientific Computing Center in Oakland, California USA and on the Tera-grid at the National Institute for Computational Science (NICS) in Tennessee USA, which is supported in part by the US National Science Foundation.

- [1] McLaughlin B M 2001 *Spectroscopic Challenges of Photoionized Plasma (ASP Conf. Series vol 247)* ed Ferland, G and Savin D W (San Francisco, CA: Astronomical Society of the Pacific) p 87
- [2] Bruch R, Rødbro M, Bisgaard P and Dahl P 1977 *Phys. Rev. Lett.* **39** 801
- [3] Rødbro M, Bruch R, Bisgaard P, Dahl P and Fastrup B 1977 *J. Phys. B: At. Mol. Phys.* **10** L483
- [4] Rødbro M, Bruch R and Bisgaard P 1979 *J. Phys. B: At. Mol. Phys.* **12** 2413
- [5] Kennedy E T and Carroll P K 1978 *J. Phys. B: At. Mol. Phys.* **11** 965
- [6] Jannitti E, Nicolosi P and Tondello G 1984 *Physica C* **124** 139
- [7] Hofmann G, Müller A, Tinschert K and Salzborn E 1990 *Z. Phys. D: Atoms, Molecules and Clusters* **16** 113
- [8] Kramida A E, Ryabtsev A N, Ekberg J O, Jink I, Mannervik S and Martinson I 2008 *Phys. Scr.* **78** 025301
- [9] Vainshtein L A and Safronova U I 1978 *At. Data Nucl. Data Tables* **21** 49
- [10] Verbockhaven G and Hansen J E 2001 *J. Phys. B: At. Mol. Opt. Phys.* **34** 2337
- [11] Chung C T and Bruch R 1983 *Phys. Rev. A* **28** 1418
- [12] Wu L and Xi J 1991 *J. Phys. B: At. Mol. Phys.* **24** 3351
- [13] Bingcong G and Wensheng D 2000 *Phys. Rev. A* **62** 032705
- [14] Fuhr J and Wiese W L 2010 *J. Phys. Chem. Ref. Data* **39** 013101
- [15] Schlachter A S, Sant'Anna M M, Covington A M, Aguilar A, Gharaibeh M F, Emmons E D, Scully S W J, Phaneuf R A, Hinojosa G, Álvarez I, Cisneros C, Müller A and McLaughlin B M 2004 *J. Phys. B: At. Mol. Opt. Phys.* **37** L103
- [16] Scully S W J, Aguilar A, Emmons E D, Phaneuf R A, Halka M, Leitner D, Levin J C, Lubell M S, Püttner R, Schlachter A S, Covington A M, Schippers S, Müller A and McLaughlin B M 2005 *J. Phys. B: At. Mol. Opt. Phys.* **38** 1967

- [17] Müller A, Schippers S, Phaneuf R A, Scully S W J, Aguilar A, Covington A M, Álvarez I, Cisneros C, Emmons E D, Gharaibeh M F, Schlachter A S, Hinojosa G, and McLaughlin B M 2009 *J. Phys. B: At. Mol. Opt. Phys.* **42** 235602
- [18] Kaastra J S and Mewe R 1993 *Astron. & Astrophys. Suppl. Ser.* **97** 443
- [19] Reilman R and Manson S T 1979 *Astrophys. J. Suppl. Ser.* **40** 815
- [20] Verner D A, Yakovlev D G, Band I M and Trzhaskovskaya M B 1993 *At. Data Nucl. Data Tables* **55** 233
- [21] Verner D A and Yakovlev D G 1995 *Astron. & Astrophys. Suppl. Ser.* **109** 125
- [22] Ferland G J, Korista K T, Verner D A, Ferguson J W, Kingdon J B and Verner E M 1998 *Pub. Astron. Soc. Pac.(PASP)* **110** 761
- [23] Ferland G J 2003 *Ann. Rev. of Astron. & Astrophys.* **41** 517
- [24] Kallman T R and Bautista M A 2001 *Astrophys. J. Suppl. Ser.* **134** 139
- [25] Cunha K, Lambert D L, Lemke M, Gies D R, Roberts L C 1997 *Astrophys. J.* **478** 211
- [26] Proffitt C R, Jönsson P, Litzién U, Pickering J C and Wahlgren G M 1999 *Astrophys. J.* **516** 342
- [27] Cunto W, Mendoza C, Ochsenbein F and Zeippen C J 1993 *Astron. & Astrophys.* **275** L5
- [28] Safronova U I and Kharitonova V N 1969 *Opt. Spectrosc* **27** 300
- [29] Goldsmith S 1974 *J. Phys. B: At. Mol. Phys.* **7** 2315
- [30] Bhatia A K 1978 *Phys. Rev. A* **18** 2523
- [31] Davis B F and Chung K T 1985 *Phys. Rev. A* **31** 3017
- [32] Scully S W J, Álvarez I, Cisneros C, Emmons E D, Gharaibeh M F, Leitner D, Lubell M S, Müller A, Phaneuf R A, Püttner R, Schlachter A S, Schippers S, Ballance C P and McLaughlin B M 2006 *J. Phys. B: At. Mol. Opt. Phys.* **39** 3957
- [33] Scully S W J, Álvarez I, Cisneros C, Emmons E D, Gharaibeh M F, Leitner D, Lubell M S, Müller A, Phaneuf R A, Püttner R, Schlachter A S, Schippers S, Ballance C P and McLaughlin B M 2007 *J. Phys. Conf. Ser.* **58** 387
- [34] Robicheaux F, Gorczyca T W, Griffin D C, Pindzola M S and Badnell N R 1995 *Phys. Rev. A* **52** 1319
- [35] Burke P G and Berrington K A 1993 *Atomic and Molecular Processes: An R-matrix Approach* (Bristol, UK: IOP Publishing)
- [36] Berrington K A, Eissner W and Norrington P H 1995 *Comput. Phys. Commun.* **92** 290 URL <http://amdpp.phys.strath.ac.uk/APAP>
- [37] Hibbert A 1975 *Comput. Phys. Commun.* **9** 141
- [38] Clementi E and Roetti C 1974 *At. Data Nucl. Data Tables* **14** 177
- [39] Ralchenko Y, Kramida A E, Reader J, and NIST ASD Team, NIST Atomic Spectra Database (version 3.1.4), National Institute of Standards and Technology, Gaithersburg, MD, USA URL <http://physics.nist.gov/asd3>
- [40] Quigley L and Berrington K A 1996 *J. Phys. B: At. Mol. Phys.* **29** 4529
- [41] Quigley L, Berrington K A and Pelan J 1998 *Comput. Phys. Commun.* **114** 225
- [42] Ballance C P, Berrington K A and McLaughlin B M 1999 *Phys. Rev. A* **60** R4217
- [43] Covington A M, Aguilar A, Covington I R, Gharaibeh M F, Shirley C A, Phaneuf R A, Álvarez I, Cisneros C, Hinojosa G, Dominguez-Lopez I, Sant'Anna M M, Schlachter A S, McLaughlin B M and Dalgarno 2002 *Phys. Rev. A* **66** 062710
- [44] Davis B F and Chung K T 1989 *Phys. Rev. A* **39** 3942
- [45] Brötz F, Trassl R, McCullough R W, Arnold W and Salzborn E 2001 *Phys. Scr.* **T92** 278
- [46] Hudson E, Shirley D A, Domke M, Remmers G, Puschmann A, Mandel T, Xue C and Kaindl G 1993 *Phys. Rev. A* **47** 361
- [47] King G C, Tronc M, Read F H, and Bradford R C 1977 *J. Phys. B: At. Mol. Phys.* **10** 2479